

## The Cancellation of Magnetic Flux. I On the Quiet Sun\*

*S. H. B. Livi*<sup>A,B</sup> *J. Wang*<sup>A,C</sup> and *S. F. Martin*<sup>A</sup>

<sup>A</sup> Solar Astronomy 264-33,  
California Institute of Technology,  
Pasadena, CA 91125, U.S.A.

<sup>B</sup> Visiting Astronomer, Instituto de Fisica,  
Universidade Federal do Rio Grande do Sul,  
Porto Alegre, Brazil.

<sup>C</sup> Visiting Associate, Beijing Observatory,  
Beijing, China.

### *Abstract*

We studied the disappearance of magnetic flux in an area of the quiet Sun from digital and photographic magnetograms recorded at 2.5 min intervals for many hours on 9 July 1984 at the Big Bear Solar Observatory. We limited the quantitative part of the analyses to features which had a total of  $10^{17}$  Mx ( $1 \text{ Mx} \equiv 10^{-8} \text{ Wb}$ ) or greater and at least a 20 G ( $1 \text{ G} \equiv 10^{-4} \text{ T}$ ) contour, and which changed by more than 10% of the maximum measured flux during the 5.5 hours of most consistent image quality during the observing day. Sixteen examples of flux disappearance and three ephemeral regions met these criteria. The disappearance of flux in these examples occurred only in closely spaced features of opposite polarity. The mutual disappearance of magnetic flux in closely spaced features of opposite polarity is herein defined as 'cancellation'. The 16 examples of cancellation were observed in combinations of network features, intranetwork features, and ephemeral regions. In two of the three ephemeral regions, an imbalance of magnetic flux between the two poles within each of the ephemeral regions was created, at least in part, by the cancellation of one pole with an adjacent feature of opposite polarity. Many smaller cancellations are clearly recognized below the threshold that we established for our initial measurements. We conclude that cancellation is the dominant way in which magnetic flux is observed to disappear on the quiet Sun.

### **1. Introduction**

Using the videomagnetograph at the Big Bear Solar Observatory, we are able to record the frequent emergence and disappearance of small magnetic features on the quiet Sun. In the time-lapse videomagnetogram films obtained, many examples are shown of both the emergence and disappearance of magnetic flux. Additionally, continuous motions and interactions take place between combinations of the strong network magnetic fields, the weak intranetwork magnetic fields and ephemeral regions. Some of these phenomena and interactions recorded in the films have been described in our previous papers (Martin 1984; Martin *et al.* 1985*a*; Wang *et al.* 1985; Zirin 1985, present issue p. 961).

Our primary emphasis in the present paper is on presenting new quantitative measures of the line-of-sight component of the magnetic flux for examples of

\* Paper presented at the R. G. Giovanelli Commemorative Colloquium, Part II, Tucson, Arizona, 17-18 January 1985.

disappearing magnetic features recorded both photographically and digitally on 9 July 1984. Our examples include the partial disappearance of the new magnetic flux from ephemeral regions. As a background, in the next section, we first present recent photographic images illustrating the appearance, disappearance, and interactions of magnetic features on the quiet Sun.

## 2. Background: The Appearance, Disappearance, and Interactions of Magnetic Flux on the Quiet Sun

The series of images in Fig. 1 reveals several typical aspects of the behaviour of magnetic features on the quiet Sun. The frames in Fig. 1 were selected from the time-lapse videomagnetogram film taken on 13 October 1984. Each frame is only a small area from the magnetograms. Zirin (1985) shows the whole field of view of the videomagnetograph on this day in Fig. 2 of his paper (see p. 964). Zirin also presents details about the videomagnetograph and the data acquisition. In Fig. 1 of our paper, the contours seen in the middle of the magnetic features are created each time the memory of the digital image processor becomes saturated. The outermost contour is estimated to be between 40 and 80 G and each successive inner contour represents higher fields by a factor of 2. The polarity of each feature is revealed by the colour outside the most external contour; positive polarity fields are white and negative are black. Each frame in Fig. 1 and subsequent figures are labelled in universal time (UT).

The initial appearance and early evolution of two ephemeral regions are shown within the ovals in Fig. 1. The first ephemeral region, F1, is one of the smallest ephemeral regions recorded to date with the videomagnetograph. At 1823, the second, larger ephemeral region is seen immediately below the first ephemeral region. The larger of the two ephemeral regions, labelled F2, is the same as feature '3' marked on Fig. 2 in Zirin's (1985) paper. The fact that the positive pole is stronger could be attributed to the previous existence of positive field at the place where the positive pole emerged. The subsequent growth in flux is readily recognized by the increase in area and in magnetic field strength of both poles.

Both ephemeral regions in Fig. 1 show the typical separation of their poles as a function of time until another magnetic feature of opposite polarity is encountered. The relative mean speed of separation in both cases was  $0.6 \text{ km s}^{-1}$ . The encounter of the negative pole of F1 with an adjacent positive fragment of magnetic flux, Z1, is seen in Fig. 1 in the frames at 1823 and 1907. At 1940, the negative poles of the two ephemeral regions begin to merge and by 2057, the two negative poles are indistinguishable. Thus, both negative poles of the ephemeral regions have encountered the same fragment of positive magnetic flux, Z1. Such encounters of small opposite polarity fragments of magnetic flux are almost always accompanied by obvious loss of magnetic flux in both of the encountering features. In this situation, the loss of flux in the positive magnetic feature is clearly seen by 2057. The loss of magnetic flux in the negative poles is masked by their merger. This example was selected for illustration because it reveals the complex interactions that often take place between magnetic features on the quiet Sun. It provides a background of the behaviour that must be taken into account when analysing the digital magnetograms illustrated in the remainder of this paper.

We do not confirm the disappearance of magnetic flux where only one polarity is involved (Topka and Tarbell 1984). We attribute the lack of confirmation to the higher

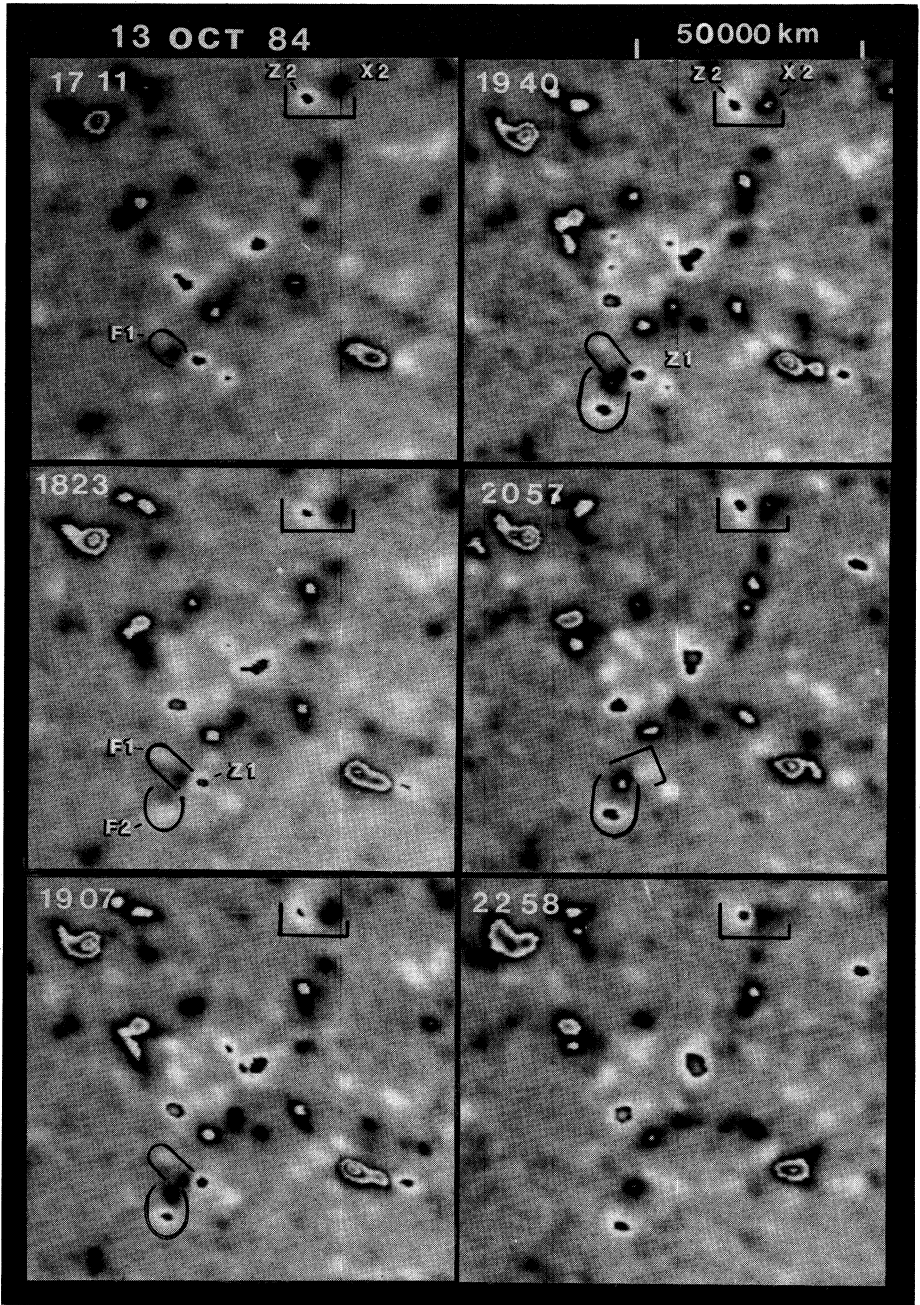


**Fig. 1.** In this videomagnetogram, the positive (white) and negative (black) polarity are identified outside of the contours. The first contour represents flux between 40 and 80 G and each successive inner contour represents a doubling of the field strength. The opposite polarity components of two ephemeral regions, F1 and F2, are seen to separate from each other. Due to this motion, the negative (black) poles of F1 and F2 encounter the adjacent fragment of positive magnetic flux Z1 at 1907 and 2057 respectively. The loss of flux in the negative poles after the encounter is masked by their merger but obvious loss of flux is seen in Z1 by 2057. Another example of opposite polarity fragments of flux approaching each other (1711–2057) and then cancelling (2258) is shown within the partial rectangle in the upper part of each frame.

magnetic sensitivity of the magnetograms that we have used in our studies. If we used magnetograms of lower sensitivity, it is clear in some situations that we might arrive at different results. For example, suppose the spatial resolution and sensitivity of the magnetograms in Fig. 1 had been less—sufficient to allow us to resolve and detect the larger, but not the smaller of the two ephemeral regions. In such a circumstance, we would have recognized only the encounter of the negative pole with the adjacent positive fragment. Then we might have erroneously concluded that the encounter resulted in the destruction of the positive flux and the simultaneous enhancement of the negative pole. Thus, our interpretation of observed flux changes should always take into account the possibility of the cancellation and merging of small fragments of magnetic flux below the threshold of detectability of the magnetograph.

For contrast with the two ephemeral regions, we also show, within the partial rectangles at the top of each frame in Fig. 1, an apparent dipolar feature. This feature initially looks similar to an ephemeral region but does not behave like one. It consists of two isolated, opposite polarity fragments, Z2 and X2, moving toward each other, a pattern of motion that has not yet been observed for any isolated ephemeral region. There is no certain change in the magnetic flux of these approaching features of opposite polarity at least until they come into contact as shown in the last frame at 2258. Because of the constancy in magnetic flux in Z2 and X2 before the last frame, these features serve as a good reference against which the ephemeral region changes and interactions can be compared.

The features described in Fig. 1 confirm our previous observations which have shown that isolated newly emerging ephemeral regions consistently exhibit properties that differ from the magnetic features that disappear (Martin *et al.* 1985*a*). Ephemeral regions do not disappear as units. Each pole individually disappears (loses magnetic flux) only when it encounters another magnetic feature of opposite polarity as illustrated in Fig. 1. Alternatively, the poles of an ephemeral region equally often encounter and merge with magnetic features of the same polarity without loss of magnetic flux. The defining characteristics of ephemeral regions are (1) appearance as a bipolar unit, (2) growth of both poles (which may be unequal if opposite polarity flux has been encountered) and (3) separation of the negative and positive pole from each other as a function of time, if opposite polarity flux has not been encountered. In contrast to these properties of ephemeral regions, the disappearance of magnetic flux on the quiet Sun is characterized by: (1) the approach of opposite polarity fragments of flux from different sources, (2) increasing magnetic field gradient between the opposite polarity fragments, which most often continues after the initial encounter, and (3) the slow and steady loss of magnetic flux in both of the encountering features. We henceforth use the term 'cancellation' to describe this type of disappearing magnetic flux. Our specific definition of cancellation is 'the mutual loss of magnetic flux in closely spaced features of opposite magnetic polarity'.

The disappearance of the line-of-sight magnetic flux in closely spaced magnetic features of opposite polarity has been previously described by Kömle (1979), Martin (1984), Martin *et al.* (1985*a*) and Wang *et al.* (1985). The properties of ephemeral regions were first described by Harvey and Martin (1973) and were further amplified by Tang *et al.* (1983) and Martin *et al.* (1985*a*).

In this paper, we use the term 'merge' only to describe magnetic features having the same polarity and which move together. Merging is accompanied by neither apparent loss nor gain in total magnetic flux of the merged features. We use the term

'encounter' only to describe opposite polarity fragments which move into apparent contact. Encounters are usually accompanied by cancellation.

The opposite polarity components of cancelling features have been shown to originate from fragments of network, ephemeral region and intranetwork magnetic fields (Martin 1984). Wang *et al.* (1985) have shown that it is convenient to label and classify cancelling features according to the origin of their components. In this paper, we use the following notation for labelling features:

Network fields	Ephemeral regions	Intranetwork fields	Unknown source
N = negative	E = neg. pole	I = negative	X = negative
P = positive	G = pos. pole	K = positive	Z = positive
	F = both poles		

Every cancelling feature is identified by a combination of two of the above letters. Additionally each letter is followed by a number which identifies each specific feature in the illustrations.

### 3. The 9 July 1984 Data from the Videomagnetograph

On 9 July 1984, continuous magnetograms were taken as on 13 October 1984 illustrated in Fig. 1. However, on this day a special effort was made to record all of the data digitally on magnetic tape as well as photographically. Two sample isogauss maps of one-quarter of the field of view of the magnetograph are shown in Fig. 2. The maps are constructed from the two digital images selected at a time interval of 2.5 hr to show the large amount of magnetic field changes that are observed during a fraction of an observing day.

Two distinct sites where the magnetic flux is disappearing at the time of the first frame in Fig. 2 are marked by partial rectangles. A new ephemeral region, F4, is enclosed in the oval in the second frame of Fig. 2. Some relatively high concentrations of intranetwork magnetic flux are labelled I1, I2, I3, I4, K1, K2, K3 and K4. The means of identification of these features by their evolution are discussed in the following sections. In this section, we discuss the general character of the data and our methods of analysing it.

This data acquired on 9 July 1984 has much better temporal resolution than was available for the previous quantitative studies (Wang *et al.* 1985). The typical interval between images was 2.5 min with several interruptions from 8 to 30 min and one longer gap of 64 min during which the calibration was made. The total series consists of 192 images recorded between 1440 UT (9 July) and 0058 UT (10 July). Each image corresponds to 2048 integrated video frame pairs. Real signal was recorded down to at least the 5 G level. The levels shown in Fig. 2 and all subsequent figures are 5, 10, 20, 40, 80, 160 and 320 G. Thicker lines are positive magnetic fields; thinner lines are negative fields. The strong network fields above 80 G are sufficiently stable that they can be correctly identified as being the same features between the early frame at 1845 and the later frame at 2114. However, even the relatively stable network features, N1 and P1, are seen to change shape. The positive feature, identified by P1, is seen to be more round in the first image and more elongated in the second. An opposite change in shape took place in N1. Initially it was elongated and had two

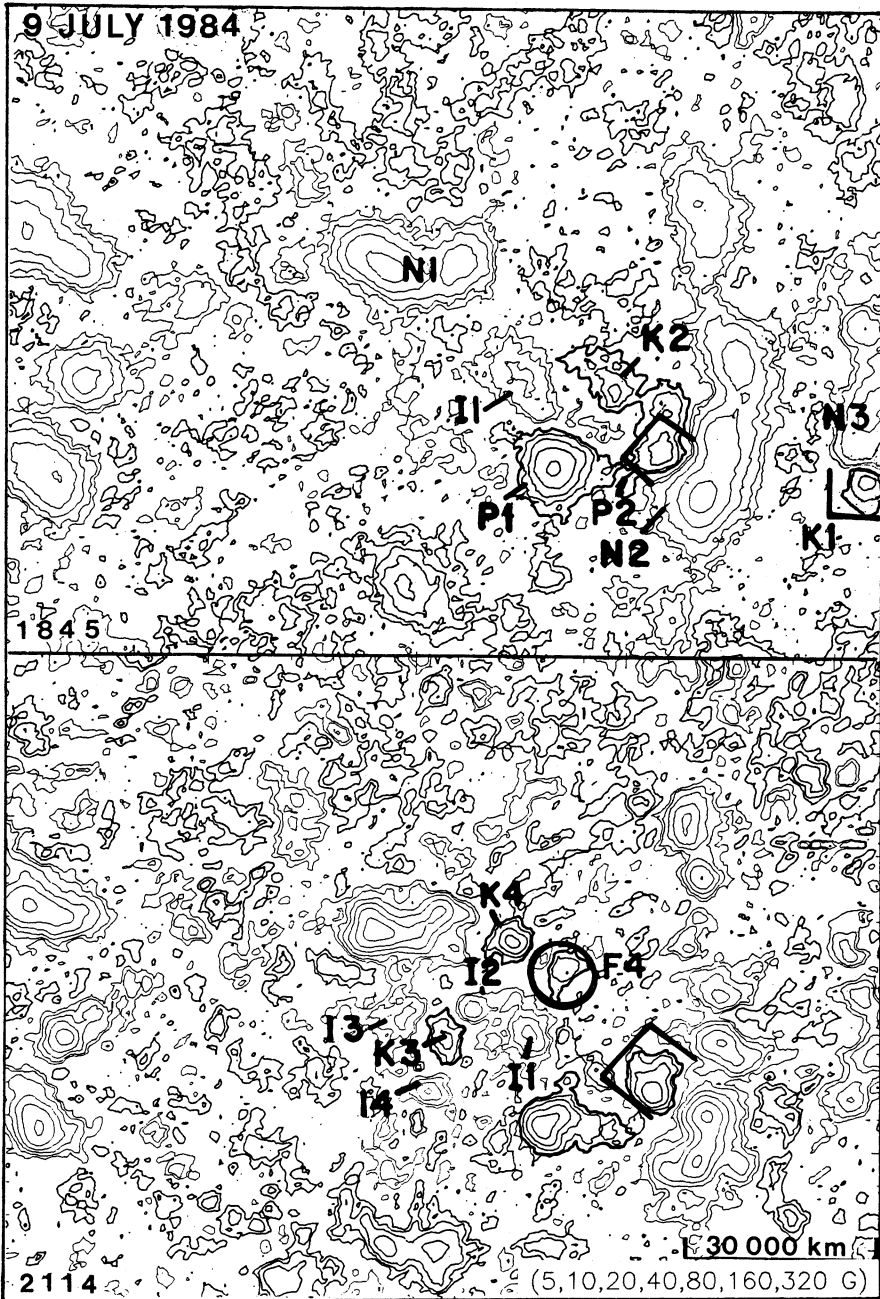


Fig. 2. These digital magnetograms show one-quarter of the total field of view used for the vidiomagnetograph at the Big Bear Solar Observatory on 9 July 1984. Positive fragments of magnetic flux are shown by thicker lines than the negative flux. Network fragments such as N1 and P1 change shape in the 2.5 hr interval between these two images, but are readily recognized at the same positions. However, in the same interval, many new intranetwork fragments form such as I2, I3, I4, K3 and K4. A new ephemeral region is enclosed within the oval. Two major sites where magnetic flux is disappearing (cancelling) are enclosed within the partial rectangles.

local maxima. By the end of the interval under study, N1 was almost round (also seen in Fig. 5 as the network fragment in the upper left corner of each frame).

We initially analysed all of the photographic images as a movie and reviewed many individual digital images to identify the magnitude of changes that could be attributed to seeing and instrumental errors. The qualitative and quantitative analyses presented in this paper were made from 90 images between 19:00 and 00:30 UT during which the data were most uniform. The changes in all features within a  $200'' \times 150''$  field of view could be consistently studied as a function of time. Even during this interval small changes over the entire images due to changes in the atmospheric image quality, the sensitivity of the magnetograms and in the balance of the opposite polarity fields could be seen. A small empirical correction was made to retain a constant ratio of positive to negative flux in the weak background fields. Another minor empirical correction was made to each of the measured images to retain approximately constant flux for the images as a whole. These corrections were made for separate research on the intranetwork magnetic fields. The corrections were found to be negligible to the results presented here because we limited the measurements in this study to the largest and most conspicuous examples of disappearing magnetic flux.

The features N1 and P1 were selected as reference features. For several hours they remained relatively isolated from other fragments of magnetic flux comparable in magnitude with the cancelling magnetic features that we selected for study. Network magnetic fields such as N1 and P1 usually do not change appreciably in total flux as long as they remain isolated from other fragments of flux. The degree of isolation is relative. On a small scale, all fragments of network are subject to continuous mergers with intranetwork magnetic flux of the same polarity and cancellation with intranetwork magnetic flux of opposite polarity (Martin 1984; Wang *et al.* 1985). After correction of the data for the changing sensitivity, P1 retained a total flux of  $(8.6 \pm 0.5) \times 10^{18}$  Mx and the total flux of N1 stayed within  $(3.1 \pm 0.1) \times 10^{19}$  Mx. The flux of P1 and N1, and all of the other features in this study, were calculated from 22 frames evenly distributed in time during the 5.5 hr interval.

In contrast to the relative stability of the network fragments in Fig. 2, it is seen that the smaller intranetwork fields, having peak contours of 5 and 10 G, are entirely changed during this interval. The sensitivity of the Big Bear videomagnetograph is sufficiently high that very weak fields of mixed polarity can be detected everywhere on the Sun as previously shown in magnetograms from Kitt Peak (Livingston and Harvey 1975; Harvey 1977; Sivaraman and Livingston 1982) and from the Lockheed Solar Observatory (Smithson 1975). Here, we do not plot fields below the 5 G level because we do not choose to discuss the nature of the intranetwork fields in this paper, aside from illustrating their role in cancellation. We need to identify their presence because the strongest intranetwork fields seen in these magnetograms develop fields on the order of 40 G or more and can become as strong as the weak ephemeral regions or small fragments of magnetic flux that split off from the more concentrated network magnetic fields. The intranetwork magnetic fields cancel and merge in the same way as the stronger magnetic fields. Some of the examples in this paper are relatively high concentrations of intranetwork magnetic fields which cancel with network magnetic fields.

During the intervals of isolation, the fluxes of the reference features P1 and N1 did not vary more than 10%. Although some of the changes are due to interaction with intranetwork magnetic fields, we attribute most of these variations to seeing,

telescope guiding errors, and changes in the transparency of the Earth's atmosphere. These effects combine together to give apparent changes in the sensitivity of the magnetograms. For example, in Fig. 3, a sensitivity change is seen from the average gain of one contour in most of the features in the frames between 2006 and 2102. To be certain that we are investigating real changes in magnetic flux, we included in the quantitative part of this study only features which initially had or developed a total flux of  $10^{17}$  Mx or greater, initially had or developed a 20 G contour, and changed by more than 10% of the maximum flux measured for each feature. The change of 10% or more was selected as a criterion because the most stable, isolated network fields, N1 and P1, did not show variations greater than 10% in 22 frames selected for their measurement during the 5.5 hr interval under study. During the 5.5 hr of data analysed, 16 conspicuous examples of disappearing magnetic features and three examples of ephemeral regions fulfilled these criteria. All of these features revealed a consistent pattern of change (either steady increase or decrease in magnetic flux and area) during many consecutive magnetograms, in contrast to the reference network features.

All of the 16 examples of disappearance happened in closely spaced opposite polarity fields and thus fit our definition of flux disappearance by cancellation. Since our initial purpose in this study is simply to accurately describe observations, we have chosen to avoid terms such as 'annihilation' or 'submergence' that would imply some physical model or knowledge of what happened to the cancelled flux. Zwaan (1978, 1984) and Parker (1984) have mentioned ways that magnetic flux can physically be removed from the photosphere.

#### 4. Examples of Cancellation of Magnetic Flux on the Quiet Sun

Fig. 3 shows the evolution of various cancelling features whose sites are labelled by partial rectangles on the second frame at 2006. The feature K5/I5 in the lower left is a typical cancelling feature. The opposite polarity fragments first move together resulting in an increasing magnetic field gradient until 2102. The beginning of the cancellation is masked by the larger degree of smearing of the features before 2006, possibly because of seeing effects. The decrease in the magnetic flux of both polarities is evident by 2219. By this time there is obvious reduction in both the area and number of contours in K5 and I5. The cancellation continues until the complete disappearance of the positive half, K5. The feature K5 reduced from  $1.0 \times 10^{18}$  Mx to below detection between 19:01 and 00:29 UT at an average rate of  $0.2 \times 10^{18}$  Mx hr<sup>-1</sup>.

The interval during which the magnetic flux is cancelling is most often recognized in these images because the magnetic field gradient at the cancellation sites usually becomes higher than between any other two features of opposite polarity. High magnetic field gradients in the range 0.01–0.03 G hr<sup>-1</sup> (Wang *et al.* 1985) are very often evidence of cancellation, although it has not been shown that all sites of high gradient are necessarily the sites of cancelling features.

The increasing gradient is evidence of the migration of unresolved magnetic structures. Without such migration during the cancellation, the magnetic field gradient would decrease rather than increase.

Concurrent with observing increasing magnetic field gradients in cancelling features, we often also observe the coalescence of adjacent flux of the same polarity. Coalescence often accompanies the migration of neighbouring magnetic flux toward a cancellation

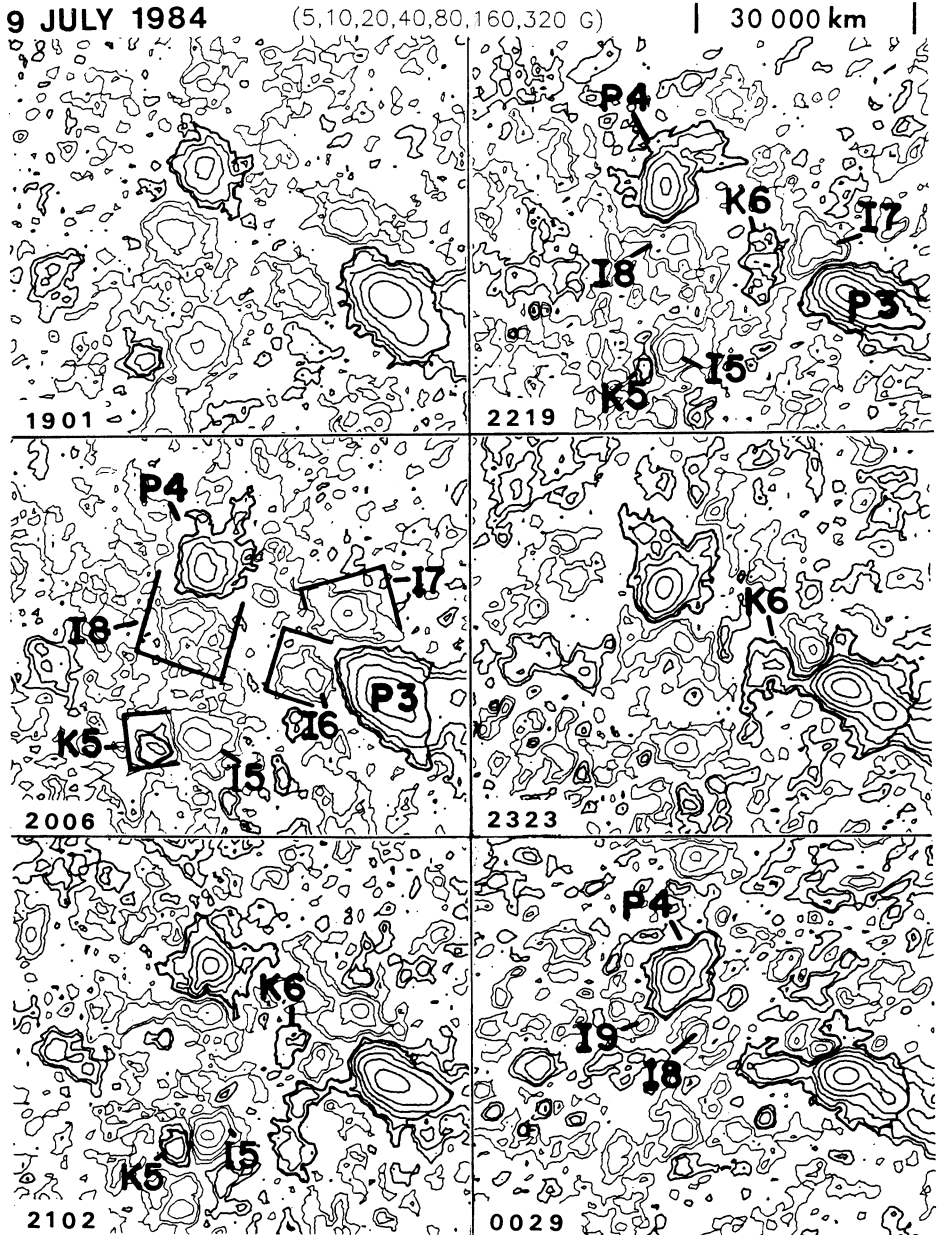


Fig. 3. Four major sites of cancellation are marked by the partial rectangles. Cancellations I6/P3 and I7/P3 involve the same positive network fragment. K5/I5 is a cancellation between intranetwork fields that continues until K5 completely disappears. I8/P4 is an example of intermittent cancellation due to the migration and changes of I8. K6 is a newly appearing fragment which resulted from the migration, coalescence, and concentration of weaker intranetwork magnetic flux.

site. In Fig. 3, I5 is a good example of the coalescence of the magnetic flux during cancellation. It becomes more compact but retains a peak field of at least 40 G throughout most of the period of cancellation with K5. The feature K5 does not show coalescence, but there is no scattered weak positive flux around K5 to coalesce with it. Hence K5 seems to disappear more rapidly than I5. Our observation of these changes indicates the desirability of understanding the nature of the fine structure of solar magnetic fields. Other examples of flux migration, coalescence, and increasing magnetic field gradients respectively within and around cancelling features are shown in Wang *et al.* (1985).

Features I6 and I7 are also cases of the simple continuous cancellation of two fragments of negative magnetic flux at adjacent sites on the border of a single larger area of positive network flux, P3; I6 disappears first around 2219 while I7 loses flux at a slower rate and has not completely disappeared by the last frame at 0029 in Fig. 3. At 1901, I7 has a flux of  $-3.0 \times 10^{18}$  Mx. By 0029, its flux has reduced to  $-0.8 \times 10^{18}$  Mx at an average rate of  $0.4 \times 10^{18}$  Mx hr<sup>-1</sup>. Feature I6 cancels faster, reducing from  $-2.1 \times 10^{18}$  Mx at 19:01 UT to  $-0.7 \times 10^{18}$  Mx at 20:47 UT, at an average rate of  $0.8 \times 10^{18}$  Mx hr<sup>-1</sup>.

Features I6 and I7 are typical cases in which the comparable loss of flux in the adjacent, larger network fragment P3 participating in the cancellation is not obvious for two reasons: (1) the loss in total flux is a small percentage change of the network fragments, and (2) network fields change shape to fill in the flux lost at cancellation sites (Wang *et al.* 1985). In these images on 9 July 1984 and most of our quiet Sun observations to date, the magnetic flux changes need to be greater than 10% of the fragments of flux involved in order to be detectable.

Left of the division between I6 and I7 is an area of increasing positive flux, labelled K6. The development of K6 is worth a brief description and comment because it represents a kind of flux change on the quiet Sun which needs to be better observed and understood. It originates from the development and merger of weak intranetwork fields. In Fig. 3, the origin of K6 is not obvious because too few frames are presented to show the evolution of this feature. In the time-lapse film, however, the negative fields of I6 and I7, as well as K6, are all seen to be concentrations of flux having their origin in the intranetwork space.

The cancellation example I8/P4 in Fig. 3 is an example in which the cancellation is not simple and continuous. The period of increasing gradient only lasts about two hours and then it decreases. The negative flux migrates to the right relative to the positive flux and splits to form two smaller concentrations of flux by 0029. Cancellation begins again with P4 for the negative knot of magnetic flux to the left, I9, as the field gradient increases between that knot and the positive fragment P4.

On the right side of the frames in Fig. 4 (1901) are two large network fragments, P5 and N4, that are cancelling. Concurrent with the decrease in flux, there is evidence in both P5 and N4 of continued migration toward each other. In P5, the centre of the highest contour gradually comes closer to the polarity inversion line. The feature N4 develops a secondary maxima which also moves toward the polarity inversion line. There is no evidence of new flux near this polarity inversion line between P5 and N4. We deduce that it is only the motion of the opposite polarities towards each other that builds the magnetic field gradient at a higher rate than can be reduced in cancellation. From the motion, we also deduce that the site of flux loss is localized at or close to the polarity inversion line.

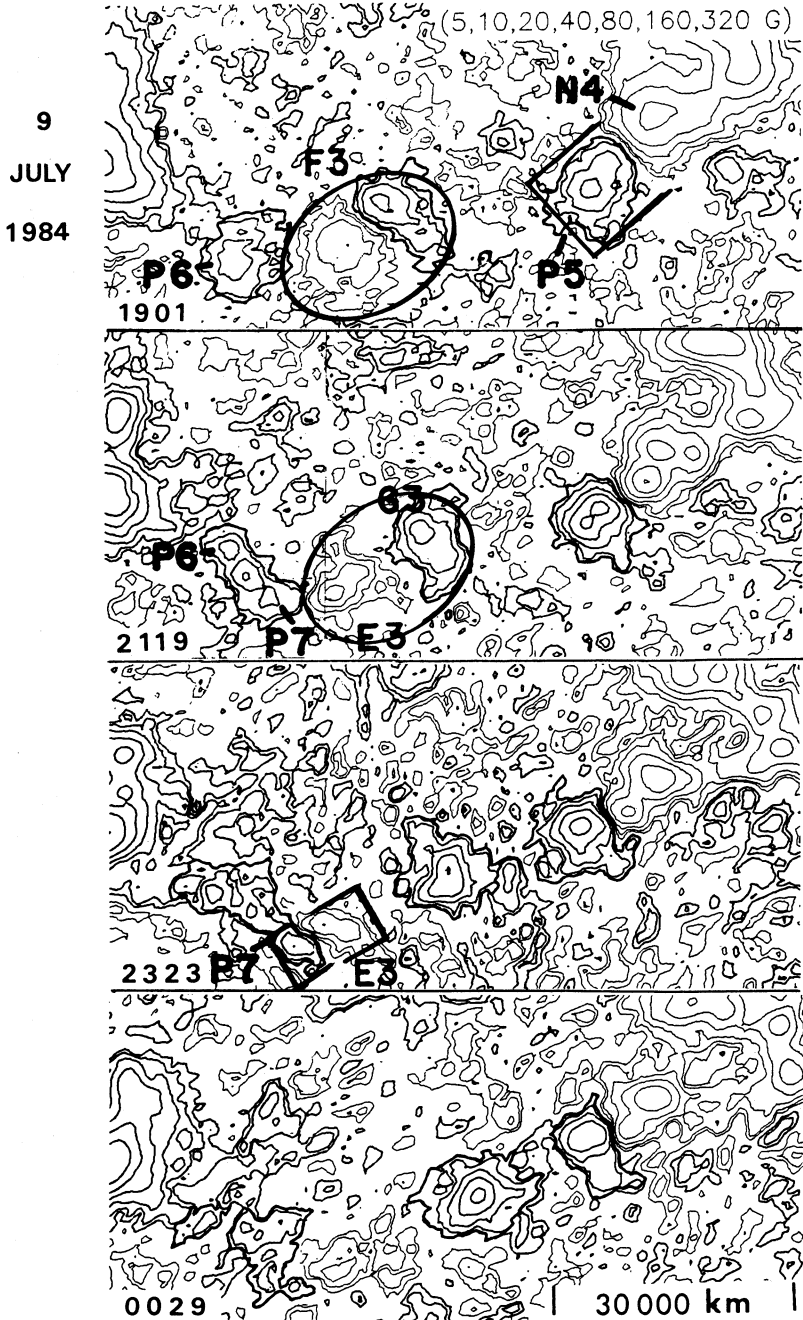


**Fig. 4.** A newly developed ephemeral region F3 is seen in the first frame. At its poles, E3 (negative) and G3 (positive) separate from each other, and E3 encounters a fragment of flux P6 that was moving toward the network fragment in the upper left of the frames. The encountered fragment splits; the upper knot, P6 continues its established migration while the lower knot, P7, begins to cancel with E3. Cancellations P7/E3 and P5/N4 show characteristic high magnetic field gradients that accompany the loss of magnetic flux.

## 5. Effects of Cancellation on Ephemeral Regions

Fig. 4 shows the development of an ephemeral region, F3, enclosed in the oval in the first frame, and a related cancellation. This ephemeral region was born between 17:22 and 18:26 UT, the largest gap in our data. At 1905 the positive flux was  $4.0 \times 10^{18}$  Mx and the negative flux was  $-4.9 \times 10^{18}$  Mx. During its subsequent growth, the more isolated positive pole G3 continued to increase in flux, while the negative pole E3 moved toward a neighbouring fragment of opposite polarity network, P6. The fragment P6 had been migrating towards another network fragment in the upper left of Fig. 4. During its migration, P6 split into two knots, P6 and P7; P6 is seen to continue the migration to the upper left, while P7 seems to be attracted to E3. Then E3 and P7 become a pronounced cancelling feature at 2323. In this example of cancellation, the decrease in flux is clearly shared by both E3 and P7 (2119). Concurrent with this mutual reduction of flux is a mutually increasing magnetic field gradient. This example very well illustrates how the magnetic field gradient at the cancellation site of one pole of an ephemeral region typically increases while the magnetic field gradient between the poles of the ephemeral region decreases. In this example, the cancellation of E3/P7 ceases by 0029. The cessation of cancellation is seen to be accompanied by a reduction of the magnetic field gradient. The feature P7 is reduced to  $0.5 \times 10^{18}$  Mx at 0029, while E3 decreased to  $-2.9 \times 10^{18}$  Mx. The loss of flux in both components of the cancellation is the same within the accuracy of our measurements. If the absolute value of the flux lost by P7 is added to the residual of E3 after cancellation, the sum is nearly the same as the flux in the non-cancelling pole of the ephemeral region G3.

**Table 1.** Magnetic fluxes (in  $10^{18}$  Mx) of ephemeral region F4 and fragment K4 identified in Fig. 5

Time	K4 (Positive)	E4 (Neg. pole)	G4 (Pos. pole)
2119	1.7	-0.42	0.48
2128	1.8	-0.9	1.3
2201	1.2	-1.1	3.2
2236	0.8	-0.8	3.2
2301	0.8	-0.6	2.1
2320	0.6	-0.4	2.0

Fig. 5 is a more drastic example of the effects of cancellation on an ephemeral region. This is the same ephemeral region F4 shown soon after its birth in Fig. 2 (2114). In Fig. 2, there is an obvious imbalance in magnetic flux between the two poles of the ephemeral region. The series of images in Fig. 5 suggests to us that the initial imbalance is due to its emergence in a background field of weak positive polarity magnetic flux. The effect of the background field can be the cancellation of some of the negative flux of F4 as it emerged and the addition of flux to the positive pole of F4. At 2119 (Fig. 5), the measured fluxes are  $-0.4 \times 10^{18}$  Mx for the negative pole and  $0.5 \times 10^{18}$  Mx for the positive pole. Adjacent to the negative pole is a positive feature K4, whose flux is  $1.7 \times 10^{18}$  Mx. The fluxes of the ephemeral region and the adjacent positive fragment K4 are given in Table 1 corresponding to the six middle frames in Fig. 5.

The degree of imbalance between the positive and negative poles of F4 increases for at least two apparent reasons: (1) cancellation of the negative pole with K4 and (2)

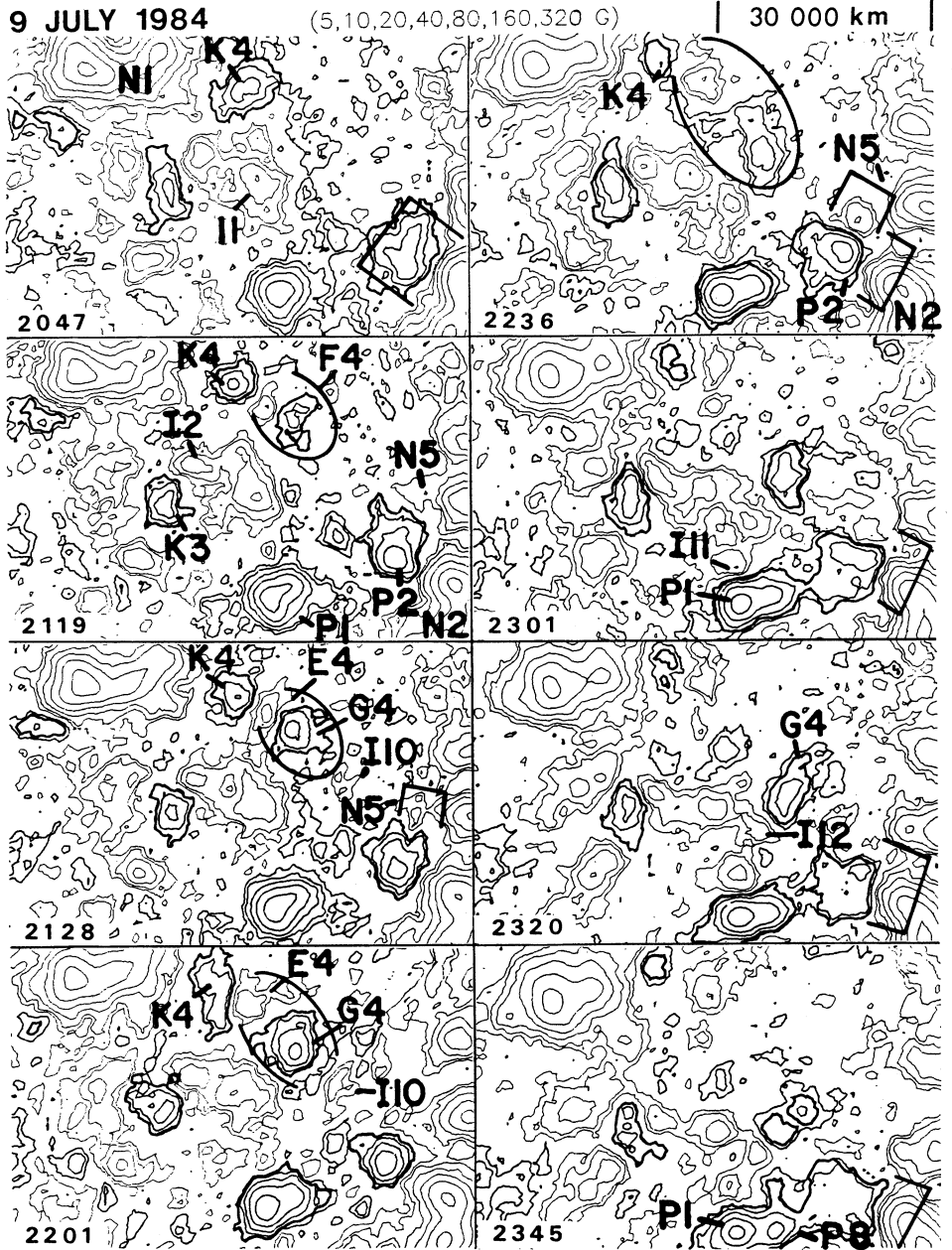


Fig. 5. As the new ephemeral region F4 grows, its negative pole E4 also is seen to cancel with intranetwork knot K4, from 2047 until 2236. The positive pole G4 merges with other positive intranetwork flux and then cancels some of its flux with negative intranetwork fragment I10. Two knots of negative flux, I11 and I12, separate from I1 and migrate respectively towards P1 and G4 to form new minor sites of cancelling magnetic flux. Intranetwork knots, I2 and K3 (2119) also form a minor cancellation site. Network knot N5 separates from a large fragment of negative network at 2119 and migrates to form a new knot cancellation site on the border of P2 (2236).

merging of the positive pole with intranetwork flux. By 2128, the negative pole E4 encounters the adjacent larger fragment of positive flux K4 and begins to cancel with it. However, the growth rate of the ephemeral region exceeds the rate of cancellation with K4. By 2128, the positive pole G4 has  $1.3 \times 10^{18}$  Mx and the negative pole  $-0.9 \times 10^{18}$  Mx. By 2201, both the positive and negative pole have reached their maximum flux, but the non-cancelling positive pole has almost three times the flux of the cancelling negative pole. In this case the positive pole has a differential gain in flux over the negative pole by much more than the flux lost in cancellation. The images in Fig. 5 suggest that this excess flux in G4 might be due to its continued merger with positive intranetwork flux as it moves away from E4. This is somewhat speculative, because G4 and whatever background positive flux it accumulated must also cancel with negative intranetwork flux such as I10. Because we have not yet shown the reliability of our measurements for the intranetwork fields, we are guessing that the interactions of G4 with intranetwork flux added more positive flux to G4 than was subtracted from it in cancellation. These observations introduce the real complexity in addressing the question of flux balance in ephemeral regions or any small-scale fields on the Sun.

The magnetic flux increase in G4 is similar to the inexplicable flux increases observed by Wilson and Simon (1983). Our observations reveal the importance of detecting and analysing the character of intranetwork magnetic flux. In Fig. 3, K6 shows that clumps of intranetwork flux alone can develop surprisingly high values of peak flux.

In Fig. 5, the poles of F4 separate as a function of time as in any typical ephemeral region. In this example, the average rate of separation was  $1.5 \text{ km s}^{-1}$ . Also, as usual for ephemeral regions, F4 stops growing at about the time that a gap of no magnetic flux develops between the two poles as seen at 2201. However, G4 continues to move away from E4. It encounters and quickly cancels the minor flux fragment I10. During this same time (after 2201), the cancellation between E4 and K4 ceases for no obvious reason. With the cessation of cancellation, the gradient of the magnetic field at the cancellation site reduces and the two previously cancelling fragments then slowly drift apart.

Previously, Martin (1984) reported that cancellation generally continues until the smaller of two cancelling features completely disappears. However, here we have shown the example of E4 in Fig. 5 in which the cancellation ceased before the complete disappearance of the smaller knot of flux K4. We ask why the cancellation sometimes ceases? Is it different because the cancellation takes place within a network cell rather than on the boundary of a cell? Is there no longer a force that drives the pole of an ephemeral region into a neighbouring fragment? Could the motion be interrupted as a consequence of magnetic reconnection? These and many other questions remain to be answered about the interactions of magnetic flux on the quiet Sun.

## 6. Cancellation and its Relationship to Transport of Magnetic Flux

In many of the cases of cancellation on 9 July 1984, the previous motion of one or both polarities were observed in the time-lapse film before the beginning of the cancellation. This motion is primarily responsible for the building of high magnetic field gradients on either side of the polarity inversion line around which the flux disappearance takes place.

In Fig. 5, it is also informative to follow the whole negative structure I1 (2047) to the left of G4 in the middle of the frames. It changes configuration continuously and stretches toward the positive neighbouring features, creating cancelling sites. It well exemplifies the interaction of fields nearly everywhere on the Sun. The movement of opposite polarities toward each other is so common that it is difficult to attribute it to pure 'random walk' of the solar photospheric fields. For example, between 1845 (Fig. 2) and 2047 (Fig. 5) part of I1 moved left to form a cancellation site I2/K3 at about 2320; another fragment I11 breaks away and moves down to cancel with P1 by 2301; yet another knot I12 moves into position to cancel with G4 around 2320. We have not attempted to measure the rate of flux disappearance in these minor examples of cancellation.

The feature N5 on the right side of the frames in Fig. 5 is another good example of the transport of flux. This event resembles the motions of the network described by Smithson (1972) as taking place in the form of sudden squirts of flux from one point to another over distances of 5000 to 20 000 km in intervals of a few hours. Numerous examples of this mode of rapid transport of flux over short distances are seen in the Big Bear Observatory magnetograms (Martin 1984; Wang *et al.* 1985; Martin *et al.* 1985*b*, present issue p. 929).

In Fig. 5, N5 is the tongue of magnetic flux that extends to the left at 2119. A 10 G contour at 2128 shows that flux has been added to the tongue which has moved further away from its source network field at 2201. The knot N5 has completely separated from its source field at 2236 and has entered into cancellation with the positive fragment P2, also associated with cancellation P2/N2. The cancellation of N5 is nearly complete by 2320. In the last frame at 2345, the remaining weak fragment of flux near the previous site of N4 is a new minor concentration of intranetwork magnetic flux that was previously moving toward N5.

The transport of flux towards an established cancellation site is common. During the cancellation P2/N2 in Fig. 5, P1 has developed a second maximum P8 (2345) that is beginning to break away from P1 and move toward the positive magnetic flux being cancelled at P2/N2. This migration of flux can result in the enhanced concentration of magnetic flux at P2/N2, the building of increased magnetic field gradients and possibly increased cancellation of the flux at P2/N2. Note the lengthening of zone of increased magnetic gradient during the cancellation at P2/N2. Also, if G4 continued its migration in its established direction, it could also merge with P2 and continue the cancellation with N2. Due to the transport of magnetic flux as in these examples, cancellation at a site can be renewed or continued.

## 7. Discussion

The average rate of flux loss for the 16 largest cancellations was  $1.1 \times 10^{18}$  Mx hr<sup>-1</sup>. The measured rates varied from  $10^{17}$  to  $4 \times 10^{18}$  Mx hr<sup>-1</sup>. In one sense the number of cancelling features and average rate of cancellation here determined could be higher than typical since the average distance between strong network fields is small. On the other hand, the number of ephemeral regions in this particular field was relatively low and this factor might result in a lower number of cancellations than on other areas of the quiet Sun. The values given here are approximate and refer to a particular region and time.

The area of the quiet Sun that we analysed has enhanced network with some well-defined cells. In the field of view there are approximately 18 supergranule cells

with an assumed average diameter of 30 000 km. The mean rate of cancellation for the major fragments of flux, having at least a 20 G contour, is  $10^{18}$  Mx per supergranule cell per hour. The mean rate of flux gain due to the birth and growth of ephemeral regions is  $0.3 \times 10^{18}$  Mx per supergranule cell per hour. Thus, it might appear that the rate of flux loss exceeded the rate of flux gain by a factor of 3 within this field of view. However, ascertaining the true net rate of flux loss or gain, even in a limited field, is a more complex problem than comparing the rates of gain and loss above an arbitrary threshold. Many of the measured cancellations were concentrations of intranetwork magnetic flux. Presumably, these cancellations are offset by an equal amount of opposite polarity concentration of flux which merged and added to the network and ephemeral regions. A more meaningful approach to determining the relative mean loss and gain of flux on an area of the quiet Sun would be to compare the flux lost only in network/network cancellations with the gain in flux in ephemeral regions. However, adequate statistical sampling of network/network cancellations would require studying a much larger field of view than obtained for this set of data on 9 July 1984. We necessarily leave to future studies the question of obtaining meaningful measures of the net gain or loss of magnetic flux on the quiet Sun at given times during the solar cycle.

The origin of some of the intranetwork concentrations was observed to be a merger of weaker intranetwork fields of the same polarity. We deduce that most of the weak intranetwork fields observed in this set of data are concentrations of yet smaller unresolved fragments of magnetic flux.

The concentrations of intranetwork magnetic flux sometimes cancelled with other intranetwork fields or ephemeral regions before further migration. Most concentrations of the intranetwork flux migrated until they met network magnetic flux and either cancelled or merged with the network flux. Because of the tendency for opposite polarity fields to migrate together, we suggest that the apparent attraction and migration of opposite polarity intranetwork and network features towards each other before and during cancellation might be a cause for the non-radial motion of some intranetwork features (Livingston and Harvey 1975).

It is interesting, and possibly informative, to note the relative rapidity of magnetic flux loss by cancellation alone. The sum of all the positive and negative flux in our field of view was  $2.2 \times 10^{21}$  Mx. At the observed mean rate of cancellation of  $1.8 \times 10^{19}$  Mx  $\text{hr}^{-1}$  for the entire field, only 120 hr or 5 days would be required to eliminate all of the flux in the field of view, under the unreal assumption that the Sun could generate only enough opposite polarity flux appropriately distributed to cancel the existing magnetic field at the observed rate. This means the rate of appearance of new flux in the form of just intranetwork concentrations and ephemeral regions is impressively high. The quiet Sun magnetic fields must constitute a large reservoir of magnetic energy.

## 8. Effects and Consequences of Cancellation

In this study we have learned that intranetwork magnetic fields quite commonly develop strong concentrations of magnetic flux yielding knots of flux having field strengths up to 40 G or more. These concentrations may last for several hours. They eventually cancel or add to the network, ephemeral regions or other intranetwork fields. We presume that equal amounts of opposite polarity intranetwork flux merge and cancel with other magnetic fields, although no systematic study has yet been

attempted. (In our data the smallest known intranetwork fields are not resolved.) If the intranetwork fields are generated and cancelled on a short time scale, these fields have no long-term net effect on the larger scale fields. However, in the short term, high concentrations of intranetwork magnetic flux might have a larger effect on the migration of network fields than previously suspected. Also, due to the merging of fields having the same polarity, some of the intranetwork fields can endure longer than previous studies have indicated (see the review by Stenflo 1976).

We have shown that cancellation can have a large effect on ephemeral regions. One of the effects of cancellation is the creation of an apparent imbalance in the magnetic flux of ephemeral regions if the ephemeral region appears at the site of pre-existing flux. The example we have shown is the ephemeral region in Fig. 4. In addition, ephemeral regions can lose a large fraction of their total flux after encounter with adjacent fragments of flux of opposite polarity. Thus, cancellation is an essential and large factor that should be accounted for in the correct measurement and calculation of the amount of magnetic flux that the Sun generates at any time in the solar cycle. This consideration applies to active regions as well as the ephemeral regions on the quiet Sun. In complexes of activity, we expect that very large amounts of magnetic flux are cancelled concurrent with its generation or emergence (Martin *et al.* 1985*b*). The situation is analogous to ephemeral regions on the quiet Sun. For simple isolated active regions, the total flux developed might be negligibly affected by cancellation during the growth phase. However, active region magnetic flux develops in complexes of activity where we expect cancellation to play a large role in the amount of measured flux and in its configuration.

The fact that ephemeral regions can cancel during their emergence implies that, in areas of strong network, one pole of small ephemeral regions might be completely cancelled in a very short time. If ephemeral regions occur with equal frequency at all longitudes on the Sun, we might expect to find a deficiency of ephemeral regions in areas of enhanced network, because the smallest ephemeral regions might be cancelled before they could be recognized. At present we do not know whether ephemeral regions have any inherent preference or lack of preference to form or emerge in the enhanced network or any other special zones on the Sun. To correctly determine any spatial preference for formation, one also needs to evaluate either the size distribution or the rate of cancellation of any ephemeral region sample.

We expect the cancellation of network magnetic fields with other network magnetic fields to have the largest effect on the long-term distribution of the residual background fields on the Sun. Any systematic migration of network fields accompanied by cancellation would slowly change the global distribution of positive and negative flux on the Sun as a whole. We speculate that the continuously changing patterns of the background fields (McIntosh 1981) are probably due in part to cancellation.

Other discussions of the importance of understanding how magnetic flux can and does disappear have been given by Zwaan (1978) and Boris *et al.* (1984).

## 9. Summary

The disappearance of magnetic flux has been studied quantitatively for quiet Sun features which had or developed at least a 20 G contour. Loss of magnetic flux was observed only at sites where opposite polarity fragments of flux had encountered one another. When the change exceeded 10% of the features measured, the flux loss could

be observed in both closely spaced features of opposite polarity. This type of mutual loss of magnetic flux in closely spaced features of opposite polarity has been defined as 'cancellation'. The mean rate of flux loss per feature in the 16 largest examples of cancellation was approximately  $10^{18} \text{ Mx hr}^{-1}$ .

Three ephemeral regions were observed from birth. In two of the three ephemeral regions, an imbalance in the magnetic flux of the poles within each region was observed to be created by the cancellation of one pole with adjacent fragments of magnetic flux of opposite polarity. In one of these examples, the imbalance was further enhanced by the merger of the other pole with intranetwork magnetic field of the same polarity.

In many cases the cancellation of flux was seen to be preceded by the transport of the magnetic flux fragments towards each other. The transport appeared to be associated with at least one of the following types of motion: (1) the convective flow of intranetwork fields from cell interiors to cell boundaries, (2) the growth and separation of the poles of ephemeral regions, (3) the migration of network, presumably along the boundaries of network cells, and (4) the direct motion of opposite polarity features towards one another.

Cancellation is commonly accompanied by a gradual increase in the gradient of the magnetic fields adjacent to the observed points of encounter of the cancelling fragments. The increasing gradients appear to be a consequence of the continued migration and coalescence of small fragments of magnetic flux towards a cancellation site.

The emergence and cancellation of magnetic flux was also observed within the intranetwork cells. The spontaneous appearance of intranetwork fields of both polarities was observed. By the merger of magnetic flux having the same polarity, the formation of concentrations of intranetwork field into fragments with fields up to 40 G or more was seen. A few of these concentrations were of the same order of magnitude as the poles of the ephemeral regions observed in the same set of data.

### Acknowledgments

We thank the Big Bear Observatory staff for the extra effort required in continuously recording the digital data analysed in this paper. S. H. B. Livi and J. Wang express their appreciation to H. Zirin for making this research possible during their respective extended visits at Caltech. S. F. Martin acknowledges the support of the Air Force Office of Scientific Research under grant AFOSR-82-0018.

### References

- Boris, J. P., DeVore, C. R., Golub, L., Howard, R., Low, B. C., Sheeley, N. R., Jr, Simon, G. W., and Tsinganos, K. C. (1984). 'Solar Terrestrial Physics—Present and Future'. Proc. NASA/NSF Solar-Terrestrial Workshop, June 1983, West Virginia (Eds B. M. Buttler and K. Papadopoulos), Ch. 3, pp. 3–18 (NASA: Washington, DC).
- Harvey, J. W. (1977). In 'Highlights of Astronomy', Vol. 4, Part II (Ed. A. E. Muller), p. 223 (Reidel: Dordrecht).
- Harvey, K. L., and Martin, S. F. (1973). *Sol. Phys.* **32**, 389.
- Kömle, N. (1979). *Sol. Phys.* **64**, 213.
- Livingston, W. C., and Harvey, J. W. (1975). *Bull. Am. Astron. Soc.* **7**, 346 (Abstract).
- McIntosh, P. S. (1981). In 'The Physics of Sunspots' (Eds L. E. Cram and J. H. Thomas), p. 7 (Sacramento Peak National Observatory: Sunspot, NM).
- Martin, S. F. (1984). Proc. Symp. on Small-scale Dynamical Processes in Quiet Stellar Atmospheres (Ed. S. L. Keil), p. 30 (National Solar Observatory: Sacramento Peak, NM).

- Martin, S. F., Livi, S. H. B., Wang, J., and Shi, Z. (1985 *a*). Proc. Workshop on Vector Magnetic Fields, May 1984, Marshall Space Flight Center, Alabama, p. 403 (NASA: Washington, DC).
- Martin, S. F., Livi, S. H. B., and Wang, J. (1985 *b*). *Aust. J. Phys.* **38**, 929.
- Parker, E. N. (1984). *Astrophys. J.* **280**, 423.
- Sivaraman, K. R., and Livingston, W. C. (1982). *Sol. Phys.* **80**, 227.
- Smithson, R. C. (1972). Ph.D. Thesis, California Institute of Technology.
- Smithson, R. C. (1975). *Bull. Am. Astron. Soc.* **7**, 346 (Abstract).
- Stenflo, J. O. (1976). In 'Basic Mechanisms of Solar Activity', IAU Symp. No. 71 (Eds V. Bumba and J. Kleczek), p. 69 (Reidel: Dordrecht).
- Tang, F., Harvey, K., Bruner, M., Kent, B., and Antonucci, E. (1983). *Adv. Space Res.* **2**, 65.
- Topka, K., and Tarbell, T. (1984). Proc. Symp. on Small-scale Dynamical Processes in Quiet Stellar Atmospheres (Ed. S. L. Keil), p. 278 (National Solar Observatory: Sacramento Peak, NM).
- Wang, J., Shi, Z., Livi, S. H. B., and Martin, S. F. (1985). *Sol. Phys.* (in press).
- Wilson, P. R., and Simon, G. (1983). *Astrophys. J.* **273**, 805.
- Zirin, H. (1985). *Aust. J. Phys.* **38**, 961.
- Zwaan, C. (1978). *Sol. Phys.* **60**, 213.
- Zwaan, C. (1984). Proc. Meeting on High Spatial Resolution in Solar Physics, September 1984, Toulouse (Ed. R. Muller), p. 263 (Springer: Berlin).

